IEEE Access
Multidisciplinary | Rapid Review | Open Access Journal

Received June 5, 2020, accepted June 20, 2020, date of publication June 30, 2020, date of current version July 20, 2020.

*Digital Object Identifier 10.1109/ACCESS.2020.3006096*

# Multi-Robot Control Inspired by Bacterial Chemotaxis: Coverage and Rendezvous via Networking of Chemotaxis Controllers

**SHINSAKU IZUMI[1], (Member, IEEE), SHUN-ICHI AZUMA[2], (Senior Member, IEEE), AND TOSHIHARU SUGIE[3], (Fellow, IEEE)**

[1]Faculty of Computer Science and Systems Engineering, Okayama Prefectural University, Okayama 719-1197, Japan
[2]Graduate School of Engineering, Nagoya University, Nagoya 464-8603, Japan
[3]Graduate School of Engineering, Osaka University, Osaka 565-0871, Japan

Corresponding author: Shinsaku Izumi (izumi@cse.oka-pu.ac.jp)

This work was supported in part by the Grant-in-Aid for Scientific Research on Innovative Areas (molecular robotics) from the Ministry of Education, Culture, Sports, Science, and Technology, Japan, under Grants 25104515 and 15H00814, and in part by the Japan Society for the Promotion of Science, Grants-in-Aid for Scientific Research, Japan, under Grants 17H03280 and 19K15016.

**ABSTRACT** This paper presents networked controllers for the coordination of multi-robot systems, inspired by the chemotaxis of bacteria. Chemotaxis is a biological phenomenon wherein each organism senses the concentration of a chemical in its environment and moves to the highest (or lowest) concentration point. The problem studied herein is a coverage problem, specifically, the problem of finding networked controllers to deploy robots so that they are located uniformly on a given space. To solve this problem, we decompose a global performance index quantifying the achieved degree of coverage into local indices that can be calculated in a distributed manner over the network of robots. By combining this with a controller causing chemotaxis, we present a solution to the coverage problem wherein each robot performs either a forward movement or random rotation based on the local performance index at each time step. Moreover, we extend this solution to rendezvous at an unspecified point. Simulation and experimental results demonstrate that our solution achieves coverage and rendezvous only via the above two types of robot movements and can handle different tasks simply by changing the global performance index, through the appropriate use of the chemotaxis controller.

**INDEX TERMS** Chemotaxis, distributed control, Escherichia coli, multi-robot systems.

## I. INTRODUCTION

### A. MOTIVATION AND CONTRIBUTIONS

The control of multi-robot systems for enabling networked robots to cooperatively execute a given task in a distributed manner has been an active research topic in the robotics, systems, and control fields. This is because multi-robot control is a key technique for realizing modern applications, such as cooperative transportation using vehicles, mobile sensor networks, and drone formation flying. In fact, these applications need control techniques such that many robots can coordinate with each other.

As a method of multi-robot control, mimicking the control algorithms of living things has been actively studied [1], [2]. For example, controllers inspired by the swarm behavior of ants [3], bees [4], and birds [5], [6] have been proposed.

The associate editor coordinating the review of this manuscript and approving it for publication was Norbert Herencsar.

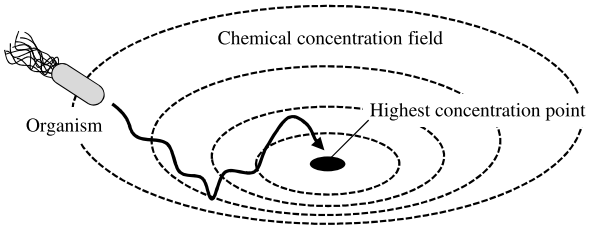


**FIGURE 1.** Chemotaxis for an attractant.

In this study, we focus on bacteria, namely *Escherichia coli* (*E. coli*), and the controller for their *chemotaxis* [7]–[9]. Chemotaxis is a biological phenomenon wherein each organism senses the concentration of a chemical in its environment and moves to the highest (or lowest) concentration point, as illustrated in Fig. 1. In such processes, each organism moves to the highest concentration point if the chemical is an attractant (*e.g.,* food) or moves to the lowest concentration point if the chemical is a repellent (*e.g.,* a toxin).

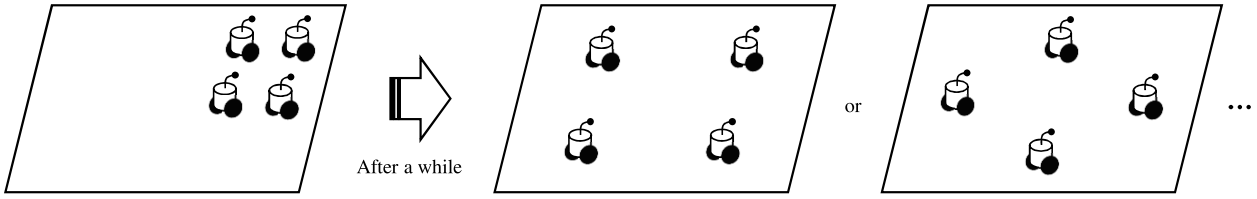


**FIGURE 2.** Coverage.

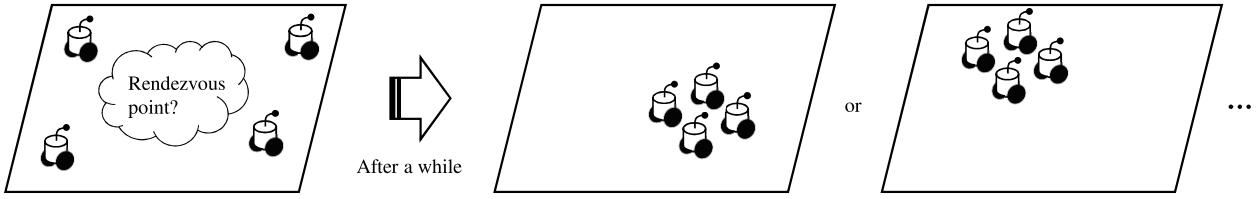


**FIGURE 3.** Rendezvous at an unspecified point.

One potential application of multi-robot control inspired by the chemotaxis of *E. coli* is substantial reduction of the costs when constructing swarm robotic systems. The chemotaxis controller of *E. coli* simply commands forward movement or random rotation, as described later, and is thus applicable to low-cost robots with limited computational resources and mobility. When constructing a large-scale system with many robots, using low-cost robots results in substantial cost reduction. Another potential application of the chemotaxis controller is the coordinating of a group of *molecular robots* [10], *i.e.,* robots composed of biomolecules. Molecular robots are necessary to realize future medical systems such as drug delivery systems using micro-robots that move inside the human body. However, we cannot directly use conventional controllers assumed to be implemented on computers as molecular robots are composed of biomolecules. A promising solution to this problem is to use controllers inspired by *E. coli* chemotaxis. *E. coli* can be thought of as molecular robots; hence, controllers whose structures are similar to theirs can be implemented in biomolecular devices. In such an application, the use of controllers inspired by other living things is difficult.

Existing studies on chemotaxis-inspired control have mainly focused on a single robot or *independent* multiple robots [11]–[18], where the chemotaxis controllers were often used for simply steering each robot to a certain point (corresponding to the highest concentration point in Fig. 1). Meanwhile, most of multi-robot applications including the aforementioned ones require multiple robots to cooperate with each other through interactions among them, for which the methods developed in existing studies are not available. This motivates us to develop *networked* chemotaxis controllers for generating the cooperative behavior of robots through such interactions. To the best of our knowledge, such networked chemotaxis controllers have never been reported.

Thus, this study aims to establish a framework of multi-robot cooperative control by networking the chemotaxis controllers of *E. coli*. As the first step, we consider coverage [19], *i.e.,* to steer robots so that they are located uniformly on a given space, as illustrated in Fig. 2. This is a fundamental task in multi-robot systems, and its applications include environment monitoring using a mobile sensor network. As shown in Fig. 2, in coverage, robots have to form a configuration depending on the situation (*e.g.,* the number of the robots and the initial configuration) while observing their neighbors. Therefore, the interactions among robots are necessary in this task, and in this sense, coverage is suitable for our purpose.

The main contributions of this study are threefold.

(i) We present networked chemotaxis controllers for coverage. In the method presented herein, each robot performs a forward movement or random rotation based on a performance index quantifying the achieved degree of coverage at each time step. The key idea of the presented method is to use the chemotaxis controller not for simply steering robots to certain points but for maximizing the performance index. By introducing the performance index determined by the positions of multiple robots and by moving each robot based on it, interactions among robots occur. In addition, by decomposing the (global) performance index into local indices that can be calculated in a distributed manner, we can obtain distributed coverage controllers inspired by the chemotaxis of *E. coli*.

(ii) We apply the aforementioned framework to rendezvous at an unspecified point [20], as illustrated in Fig. 3, to demonstrate that it can handle tasks other than coverage. Rendezvous is also a fundamental task in multi-robot systems, and its applications include resource collection using vehicles. We first show that rendezvous has a property similar to that of coverage with respect to the decomposition of the performance index described above. Based on this, networked chemotaxis controllers for rendezvous are presented.

(iii) In addition to numerical simulations, we conduct experiments using mobile robots to verify the

**TABLE 1. Relation between this study and related studies.**

| | | | | |
|---|---|---|---|---|
| Chemotaxis-inspired approaches | | | Specific signals from the environment | |
| | | | Necessary | Not necessary |
| | Complexity of methods | Increases with $n$ | [27] | [25], [26] |
| | | Does not increase with $n$ | [23], [24] | This study |
| Control theory-based approaches (for unicycle-type robots) | | | Information on robots necessary for control | |
| | | | Positions and orientations | Positions only |
| | Control input to each robot | Continuous-valued | [19], [30]–[37] | |
| | | A few discrete values | | This study |

effectiveness of the proposed networked controllers. The results show that the proposed controllers are effective even for actual robots with some hardware constraints and are feasible in a real setting.

### B. RELATED WORK

Chemotaxis has been actively studied in several research fields. For instance, in computational systems biology, a gene regulatory network model for generating chemotaxis was proposed [21]. In the robotics and systems fields, various applications of chemotaxis controllers have been reported, *e.g.,* source seeking [11]–[18], target search and trapping [22], coverage [23], [24], pattern formation [25], [26], aggregation [27], and sorting [28], [29]. Among these studies, [23]–[27] addressed tasks similar to those in this study. Oyekan *et al.* [23], [24] proposed coverage control methods to deploy robots such that the distribution of the robots corresponds to that of a hazardous substance in the environment for surveillance. However, because they assumed that each robot could receive the concentration signal of the substance to move toward its desired position, their methods are not applicable to our coverage problem, in which such a concentration signal is not available. In [25], [26], methods for pattern formation were developed by designing a function describing a virtual chemical concentration field via genetic programming. However, the complexity of these methods increases with the number of robots because genetic programming requires many simulations of the entire system. This makes the application of these methods to large-scale systems difficult. In contrast, the complexity of our method is determined not by the number of robots but by the number of their neighbors. In [27], an aggregation method based on reaction–diffusion processes was developed, where spatial waves traveling on the ground are generated and robots move toward the wave sources. However, this method requires a system for generating the waves and is therefore not applicable to our rendezvous problem without it. These differences are summarized in the upper half of Table 1, where $n$ is the number of robots. In addition, from a technical viewpoint, the above-mentioned studies used chemotaxis controllers to steer robots to certain points, whereas we use the chemotaxis controller to maximize the performance index for the task.

On the other hand, in the field of control theory, a number of researchers have studied coverage [19], [30]–[33] and rendezvous [34]–[37] for multi-robot systems. They considered unicycle-type robots similar to those used in this study and proposed controllers using information on the positions and orientations of the robots. In contrast, our controllers require the information only on the positions of robots. Moreover, in their methods, the control input to each robot should be a continuous-valued signal, whereas we use only a few discrete values (*i.e.,* extremely low resolution) as the control input. These differences are summarized in the lower half of Table 1.

As presented in Table 1, we would like to emphasize that this study presents solutions to coverage and rendezvous problems subject to the following four conditions, unlike in the existing studies:

(i) The presence of specific signals (such as concentration signals of substances) is not assumed for the environment.
(ii) The complexity of the solution does not increase with the number of robots.
(iii) The position information of the (neighboring) robots is the only information available to the controller of each robot.
(iv) The control input to each robot can only take one of a few discrete values.

Conditions (i) and (ii) broaden the application of the proposed controllers. Conditions (iii) and (iv) allow us to use the proposed controllers for robots with limited sensing capabilities and mobility, resulting in cost reduction.

Simple controllers for coverage can be found in [38]. The coverage controllers are based on a computation-free concept and determine the action of each robot from only a single bit of information, *i.e.,* whether another robot is present in its line of sight. However, the coverage controllers are designed using a black-box optimization method that requires many simulations of the entire system; thus, the complexity of the design process increases with the number of robots. In addition, using the black-box optimization method may make intuitive understanding of the behavior of the resulting controllers difficult. In contrast, the core idea of our method is to move robots so as to increase the performance index for the task using the chemotaxis controller, which can be easily understood. Consequently, we can handle another task simply by replacing the performance index for coverage with that for the task, as demonstrated in this paper.

Next, we discuss the relation between this study and the game-theoretic approach proposed in [39]. We use the idea of potential games to decompose the performance indices for coverage and rendezvous. However, the resulting controllers are different from those developed in [39]. In [39], only a randomly chosen robot (or a randomly chosen group of robots) is allowed to update its actions at each time step, which requires a supervisor. Moreover, before updating its action, the chosen robot has to select a trial action and calculate the local performance index that would result if it was performed. This may be impossible for robots with limited sensing capability because they cannot obtain information regarding distant locations without moving. In contrast, our controllers do not require any supervisor nor calculation of the local performance indices for virtual actions.

Finally, we explain the differences between this study and our related studies [40], [41]. This study is based on [40] in conference proceedings, but provides new ideas and results. First, we introduce the concept of the decomposition of the performance indices for tasks as a generalization of the idea proposed in [40], which addressed only coverage. As a result, the proposed framework can handle other tasks as well as coverage by finding performance indices that can be decomposed. Second, to demonstrate this, we present networked chemotaxis controllers for rendezvous at an unspecified point using the concept of decomposition. Third, through experiments conducted using mobile robots, we demonstrate that the proposed controllers can be used in a real setting. Meanwhile, [41] is based on a part of the results in this study, wherein this paper is cited as a submitted paper. However, the purpose of [41] is different from that of this study. In [41], we considered formation control and investigated the effects of two types of chemotaxis controllers on the accuracy of the resulting formation, whereas this study aims to establish a fundamental framework to generate the cooperative behavior of robots through the interactions by the networking of the chemotaxis controllers.

### C. NOTATION

The major notations used throughout this paper are listed in Table 2. The upper half summarizes the standard mathematical symbols, and the lower half summarizes major symbols in this paper. In addition, for the vectors $\boldsymbol{v}_1, \boldsymbol{v}_2, \ldots, \boldsymbol{v}_m \in \mathbb{R}^2$ and the set $\mathbb{J} := \{j_1, j_2, \ldots, j_\ell\} \subseteq \{1, 2, \ldots, m\}$, we define $[\boldsymbol{v}_j]_{j\in\mathbb{J}} := [\boldsymbol{v}_{j_1}^\top \ \boldsymbol{v}_{j_2}^\top \ \cdots \ \boldsymbol{v}_{j_\ell}^\top]^\top \in \mathbb{R}^{2\ell}$. For example, $[\boldsymbol{v}_j]_{j\in\mathbb{J}} := [\boldsymbol{v}_1^\top \ \boldsymbol{v}_4^\top]^\top$ for $\boldsymbol{v}_1, \boldsymbol{v}_2, \ldots, \boldsymbol{v}_5$ and $\mathbb{J} := \{1, 4\}$.

## II. PROBLEM FORMULATION

Consider the multi-robot system shown in Fig. 4, which is composed of $n$ robots.

Robot $i$ ($i \in \{1, 2, \ldots, n\}$) is a discrete-time model of a two-wheeled mobile robot described by

$$\begin{bmatrix} \boldsymbol{x}_i(t+1) \\ \theta_i(t+1) \end{bmatrix} = \begin{bmatrix} \boldsymbol{x}_i(t) \\ \theta_i(t) \end{bmatrix} + \begin{bmatrix} \cos(\theta_i(t) + u_{i2}(t))u_{i1}(t) \\ \sin(\theta_i(t) + u_{i2}(t))u_{i1}(t) \\ u_{i2}(t) \end{bmatrix}, \quad (1)$$

**TABLE 2. Major notations used throughout this paper.**

| Symbol | Definition |
|---|---|
| $\mathbb{R}$ | Real number field |
| $\mathbb{R}_+$ | Set of positive real numbers |
| $\mathbb{R}_{0+}$ | Set of nonnegative real numbers |
| $\mathbf{0}$ | Zero vector |
| $\|\boldsymbol{v}\|$ | Euclidean norm of the vector $\boldsymbol{v}$ |
| $\|\mathbb{S}\|$ | Cardinality of the set $\mathbb{S}$ |
| $\mathbb{B}(\boldsymbol{c}, r)$ | Closed disk of radius $r$ centered at $\boldsymbol{c}$, *i.e.*, $\mathbb{B}(\boldsymbol{c}, r) := \{\boldsymbol{p} \in \mathbb{R}^2 \mid \|\boldsymbol{p} - \boldsymbol{c}\| \leq r\}$ |
| $n$ | Number of robots |
| $i$ | Robot index |
| $\boldsymbol{x}_i$ | Translational position of robot $i$ |
| $\theta_i$ | Rotational position of robot $i$ |
| $\boldsymbol{u}_i$ | Control input to robot $i$ |
| $t$ | Discrete time |
| $\mathbb{N}_i$ | Index set of the neighbors of robot $i$ |
| $J$ | (Global) performance index |
| $J_i$ | Local performance index |

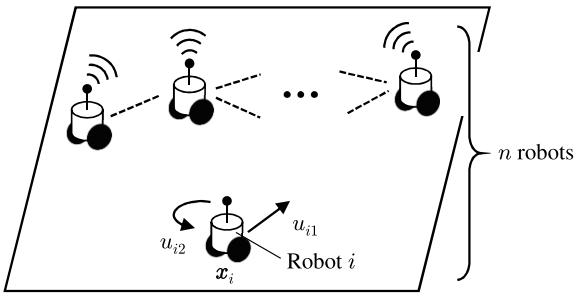


**FIGURE 4. Multi-robot system.**

where $\boldsymbol{x}_i(t) \in \mathbb{R}^2$ and $\theta_i(t) \in \mathbb{R}$ are its translational and rotational positions and $u_{i1}(t) \in \mathbb{R}$ and $u_{i2}(t) \in \mathbb{R}$ are the control inputs corresponding to the translational and rotational velocities, respectively.

A local controller is assumed to be embedded in each robot. The local controller of robot $i$ is given by

$$L_i : \begin{cases} \boldsymbol{\xi}_i(t+1) = \boldsymbol{g}_1(\boldsymbol{\xi}_i(t), [\boldsymbol{x}_j(t)]_{j\in\mathbb{N}_i(t)}), \\ \boldsymbol{u}_i(t) = \boldsymbol{g}_2(\boldsymbol{\xi}_i(t), [\boldsymbol{x}_j(t)]_{j\in\mathbb{N}_i(t)}), \end{cases} \quad (2)$$

where $\boldsymbol{\xi}_i(t) \in \mathbb{R}^m$ is the state (corresponding to a memory), $[\boldsymbol{x}_j(t)]_{j\in\mathbb{N}_i(t)} \in \mathbb{R}^{2|\mathbb{N}_i(t)|}$ is the input, $\boldsymbol{u}_i(t) \in \mathbb{R}^2$ is the output, *i.e.*, $\boldsymbol{u}_i(t) := [u_{i1}(t) \ u_{i2}(t)]^\top$, and $\boldsymbol{g}_1 : \mathbb{R}^m \times \mathbb{R}^{2|\mathbb{N}_i(t)|} \to \mathbb{R}^m$ and $\boldsymbol{g}_2 : \mathbb{R}^m \times \mathbb{R}^{2|\mathbb{N}_i(t)|} \to \mathbb{R}^2$ are functions determining the controller structure. The set $\mathbb{N}_i(t) \subseteq \{1, 2, \ldots, n\}$ is the index set of the *neighbors* of robot $i$, *i.e.*, the robots whose positional information is available to robot $i$. The functions $\boldsymbol{g}_1$ and $\boldsymbol{g}_2$ and the initial state $\boldsymbol{\xi}_i(0)$ are assumed to be the same for all the robots. This implies that all robots are treated in the same manner, guaranteeing that the entire system is scalable. For simplicity, we assume $\boldsymbol{\xi}_i(0) := \mathbf{0}$.

The neighbor set is of the form

$$\mathbb{N}_i(t) := \{j \in \{1, 2, \ldots, n\} \mid \boldsymbol{x}_j(t) \in \mathbb{B}(\boldsymbol{x}_i(t), r)\}, \quad (3)$$

where $r \in \mathbb{R}_+$ is the communication/sensing range. Equation (3) represents an $r$-disk proximity network, in which each robot can obtain information on its own position and those of robots within radius $r$. This corresponds to a situation in which each robot has, for example, a GPS receiver and a wireless communication unit or a stereo camera.

Next, the coverage problem is formulated. Let us introduce the following performance index [42]:

$$J(\boldsymbol{x}) := \int_{\mathbb{Q}\cap(\cup_{i=1}^{n}\mathbb{B}(\boldsymbol{x}_i, r/2))} 1\, d\boldsymbol{q}, \tag{4}$$

where $\boldsymbol{x} := [\boldsymbol{x}_1^\top\ \boldsymbol{x}_2^\top\ \cdots\ \boldsymbol{x}_n^\top]^\top$ and $\mathbb{Q} \subset \mathbb{R}^2$ is a space to be covered by $n$ robots. This expresses the area of the union of the disks $\mathbb{B}(\boldsymbol{x}_i, r/2)$ $(i = 1, 2, \ldots, n)$ in the set $\mathbb{Q}$. Thus, maximizing $J(\boldsymbol{x})$ means coverage in the sense that each robot is located at a certain distance from the others. Then, let us consider the following problem.

*Problem 1:* For the multi-robot system shown in Fig. 4, suppose that a coverage space $\mathbb{Q} \subset \mathbb{R}^2$ is given. Find local controllers $L_1, L_2, \ldots, L_n$ (*i.e.,* functions $\boldsymbol{g}_1$ and $\boldsymbol{g}_2$) such that

$$\lim_{t\to\infty} J(\boldsymbol{x}(t)) = \max_{\boldsymbol{x}\in\mathbb{R}^{2n}} J(\boldsymbol{x}) \tag{5}$$

for every initial state $(\boldsymbol{x}_i(0), \theta_i(0)) \in \mathbb{Q} \times \mathbb{R}$ $(i = 1, 2, \ldots, n)$.

*Remark 1:* We suppose that the robots *cooperatively* cover the target space $\mathbb{Q}$ while observing their neighbors. Hence, any local controllers whose inputs do not depend on the positions of the neighbors cannot be a solution to Problem 1. This means that an appropriate combination of the chemotaxis controller and information on the positions of the neighbors is necessary to obtain a chemotaxis-inspired solution to the problem. In this sense, Problem 1 is challenging.

## III. MATHEMATICAL MODEL OF E. COLI CHEMOTAXIS

To explain our solution to Problem 1, this section provides a mathematical model [43] of the chemotaxis of *E. coli*.

### A. CHEMOTAXIS OF E. COLI

As described in Section I-A, chemotaxis is a biological phenomenon wherein each organism senses the concentration of a chemical in its environment and moves to the highest (or lowest) concentration point. The chemotaxis controller of *E. coli* causes this phenomenon in the following manner. Consider an *E. coli* in a chemical concentration field with an attractant (see Fig. 1). If the concentration at the current position is higher than that at the previous position, the chemotaxis controller commands forward movement, considering that the resulting position might be a higher concentration point. Conversely, if the concentration at the current position is lower than that at the previous position, the chemotaxis controller commands random rotation to prevent the *E. coli* from going to a lower concentration point. In this manner, a biased random walk to the highest concentration point occurs, allowing the *E. coli* to reach it.

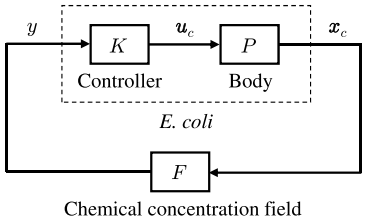


**FIGURE 5.** Feedback system representing *E. coli* chemotaxis.

### B. MATHEMATICAL MODEL [43]

The chemotaxis of *E. coli* can be modeled as the feedback system shown in Fig. 5. This system is composed of an *E. coli* and the chemical concentration field $F$, and the *E. coli* is expressed as a combination of its body $P$ and controller $K$.

The physical dynamics of the body $P$ is described by

$$\begin{bmatrix}\boldsymbol{x}_c(t+1)\\ \theta_c(t+1)\end{bmatrix} = \begin{bmatrix}\boldsymbol{x}_c(t)\\ \theta_c(t)\end{bmatrix} + \begin{bmatrix}\cos(\theta_c(t)+u_{c2}(t))u_{c1}(t)\\ \sin(\theta_c(t)+u_{c2}(t))u_{c1}(t)\\ u_{c2}(t)\end{bmatrix}, \tag{6}$$

where $\boldsymbol{x}_c(t) \in \mathbb{R}^2$ and $\theta_c(t) \in \mathbb{R}$ are the translational and rotational positions of the *E. coli* and $u_{c1}(t) \in \mathbb{R}$ and $u_{c2}(t) \in \mathbb{R}$ are the control inputs corresponding to the translational and rotational velocities, respectively.

The controller $K$ is given by

$$K: \begin{cases} \xi_c(t+1) = y(t), \\ \boldsymbol{u}_c(t) = \begin{cases} \begin{bmatrix} v \\ 0 \end{bmatrix} & \text{if } \xi_c(t) \le y(t), \\ \begin{bmatrix} v \\ \frac{2}{3}\pi \end{bmatrix} & \text{if } \xi_c(t) > y(t),\ w(t) = 1, \\ \begin{bmatrix} v \\ -\frac{2}{3}\pi \end{bmatrix} & \text{if } \xi_c(t) > y(t),\ w(t) = -1, \end{cases} \end{cases} \tag{7}$$

where $\xi_c(t) \in \mathbb{R}$ is the state (corresponding to a memory), $y(t) \in \mathbb{R}_{0+}$ is the input, $\boldsymbol{u}_c(t) \in \mathbb{R}^2$ is the output, *i.e.,* $\boldsymbol{u}_c(t) := [u_{c1}(t)\ u_{c2}(t)]^\top$, $v \in \mathbb{R}_+$ is a constant number, and $w(t) \in \{-1, 1\}$ is a random number that follows a Bernoulli distribution with equal-probability binary variables (*i.e.,* 1 and $-1$). The initial state $\xi_c(0)$ is assumed to be zero.

The chemical concentration field $F$ is of the form

$$F: y(t) = f(\|\boldsymbol{x}_c(t)\|), \tag{8}$$

where $\boldsymbol{x}_c(t)$ is the input, $y(t)$ is the output, that is, the concentration at the position $\boldsymbol{x}_c(t)$, and $f: \mathbb{R}_{0+} \to \mathbb{R}_{0+}$ is a function characterizing $F$.

In the feedback system shown in Fig. 5, the controller $K$ operates as follows. From $\xi_c(t) = y(t-1)$ because of (7), the concentration $y(t-1)$ at the previous position is stored in the state $\xi_c(t)$. Hence, $\xi_c(t) \le y(t)$ indicates that the concentration at the current position is higher than or equal to that at the previous position. In this case, the controller

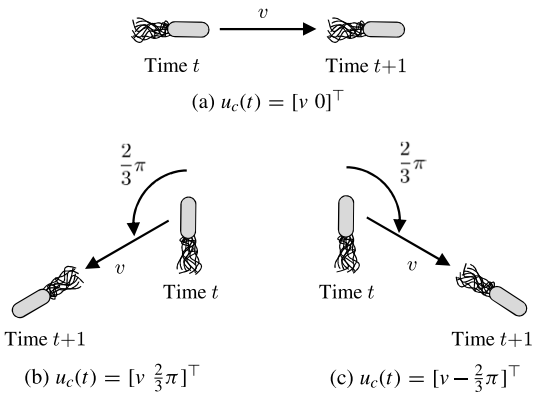


**FIGURE 6.** Movements commanded by the controller $K$.

$K$ commands straight movement, as shown in Fig. 6 (a). In contrast, $\xi_c(t) > y(t)$ indicates that the concentration at the current position is lower than that at the previous position. In this case, $K$ commands a combination of rotational and straight movements, as shown in Figs. 6 (b) and (c). The direction of the rotation is randomly chosen by $w(t)$. For this controller $K$, Azuma *et al.* [43] obtained a convergence result in a stochastic sense by showing that a Lyapunov-like function is decreasing.

We provide an example to demonstrate the performance of the controller $K$. For the feedback system shown in Fig. 5, let $v := 0.3$ and

$$f(\|\boldsymbol{x}_c\|) := 2e^{-0.01\|\boldsymbol{x}_c\|^2}, \tag{9}$$

for which the origin is the highest concentration point. Fig. 7 shows a sample trajectory of the system for $(\boldsymbol{x}_c(0), \theta_c(0)) := ([-5\ \ -6]^\top, (2/3)\pi)$, where the ellipsoids represent the positions of the body and the circles and arcs represent the contour lines of $f(\|\boldsymbol{x}_c\|)$. The body moves to an area around the highest concentration point.

## IV. COVERAGE VIA NETWORKING OF Chemotaxis CONTROLLERS

In this section, we present a solution to Problem 1.

### A. DECOMPOSITION OF PERFORMANCE INDEX

As stated in Section III-B, an *E. coli* reaches the highest concentration point for a chemical via the chemotaxis controller $K$. That is, $K$ plays the role of steering the *E. coli* toward the maximum point of the function $f$ in (8). Hence, in order to satisfy (5), we propose to use $K$ for each local controller $L_i$, where we regard each robot and the performance index $J$ in (4) as an *E. coli* and $f$, respectively.

However, this method cannot be directly implemented because calculating the value of $J$ requires information on the positions of all the robots, but each robot can only obtain information about the positions of its neighbors. To overcome this problem, we introduce the concept of the *decomposition* of $J$. Local performance indices $J_i$ $(i = 1, 2, \ldots, n)$ are said to be a decomposition of $J$ if each $J_i$ satisfies the following two conditions.

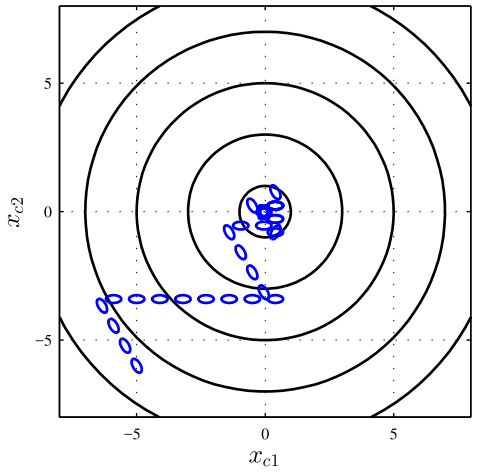


**FIGURE 7.** Sample trajectory of the feedback system shown in Fig. 5.

(C1) The value of $J_i$ can be calculated from the positions of the neighbors of robot $i$.
(C2) $J$ increases if $J_i$ increases.

The first condition guarantees that $J_i$ is available to the local controller $L_i$ in (2), which overcomes the above-mentioned problem. The second condition implies that increasing each $J_i$ will result in satisfying (5). We use such $J_i$ $(i = 1, 2, \ldots, n)$ instead of $J$.

Based on this idea, the following local performance indices are introduced:

$$J_i([\boldsymbol{x}_j]_{j\in\mathbb{N}_i}) := \int_{\mathbb{Q}\cap(\cup_{j\in\mathbb{N}_i}\mathbb{B}(\boldsymbol{x}_j, r/2))} 1\, d\boldsymbol{q} - \int_{\mathbb{Q}\cap(\cup_{j\in\mathbb{N}_i\setminus\{i\}}\mathbb{B}(\boldsymbol{x}_j, r/2))} 1\, d\boldsymbol{q} \quad (i = 1, 2, \ldots, n). \tag{10}$$

Then, the following result is obtained.

*Theorem 1:* Consider the performance index $J$ in (4) and the local performance index $J_i$ in (10). Then, the following statements hold.

(i) Condition (C1) holds for every $i \in \{1, 2, \ldots, n\}$.
(ii) The relation

$$J(\overline{\boldsymbol{x}}(i, \boldsymbol{z})) - J(\boldsymbol{x}) = J_i(\overline{[\boldsymbol{x}_j]}_{j\in\mathbb{N}_i}(i, \boldsymbol{z})) - J_i([\boldsymbol{x}_j]_{j\in\mathbb{N}_i}) \tag{11}$$

holds for every $i \in \{1, 2, \ldots, n\}$, where $\overline{\boldsymbol{x}}(i, \boldsymbol{z}) \in \mathbb{R}^{2n}$ is $\boldsymbol{x}$ in which $\boldsymbol{x}_i$ is replaced with $\boldsymbol{z}$, and $\overline{[\boldsymbol{x}_j]}_{j\in\mathbb{N}_i}(i, \boldsymbol{z}) \in \mathbb{R}^{2|\mathbb{N}_i|}$ is similarly defined.

*Proof:* From (10), (i) is trivial. On the other hand, (ii) can be proven as follows. The neighbor set (3) implies that $J_i$ expresses the area of the region that is only covered by robot $i$, that is,

$$J_i([\boldsymbol{x}_j]_{j\in\mathbb{N}_i}) = \int_{\mathbb{Q}\cap(\cup_{j=1}^n\mathbb{B}(\boldsymbol{x}_j, r/2))} 1\, d\boldsymbol{q} - \int_{\mathbb{Q}\cap(\cup_{j\neq i}\mathbb{B}(\boldsymbol{x}_j, r/2))} 1\, d\boldsymbol{q}. \tag{12}$$

From (4) and (12), we have

$$J(\boldsymbol{x}) = J_i([\boldsymbol{x}_j]_{j\in\mathbb{N}_i}) + \int_{\mathbb{Q}\cap(\cup_{j\neq i}\mathbb{B}(\boldsymbol{x}_j, r/2))} 1\, d\boldsymbol{q}. \tag{13}$$

Equation (13) yields (11) because the second term of the right-hand side is independent of $\boldsymbol{x}_i$. Hence, (ii) holds. ■

In Theorem 1, (ii) means that when only robot $i$ moves, $J_i$ increases or decreases as much as $J$ does. In this sense, $J_i$ satisfies condition (C2). This and (i) indicate that $J_i$ $(i = 1, 2, \ldots, n)$ are a decomposition of $J$.

### B. PROPOSED CONTROLLERS

From the above results and the chemotaxis controller $K$ in (7), we propose the following solution to Problem 1:

$$g_1(\xi_i(t), [\boldsymbol{x}_j(t)]_{j\in\mathbb{N}_i(t)}) := J_i([\boldsymbol{x}_j(t)]_{j\in\mathbb{N}_i(t)}), \tag{14}$$

$$\boldsymbol{g}_2(\xi_i(t), [\boldsymbol{x}_j(t)]_{j\in\mathbb{N}_i(t)}) := \begin{cases} \begin{bmatrix} v \\ 0 \end{bmatrix} & \text{if } \xi_i(t) \le J_i([\boldsymbol{x}_j(t)]_{j\in\mathbb{N}_i(t)}), \\ \begin{bmatrix} v \\ \frac{2}{3}\pi \end{bmatrix} & \text{if } \xi_i(t) > J_i([\boldsymbol{x}_j(t)]_{j\in\mathbb{N}_i(t)}),\ w_i(t) = 1, \\ \begin{bmatrix} v \\ -\frac{2}{3}\pi \end{bmatrix} & \text{if } \xi_i(t) > J_i([\boldsymbol{x}_j(t)]_{j\in\mathbb{N}_i(t)}),\ w_i(t) = -1, \end{cases} \tag{15}$$

where $\xi_i(t)$ is a scalar, *i.e.,* $m := 1$ (and thus non-bold $g_1$ and $\xi_i(t)$ are used), and $w_i(t) \in \{-1, 1\}$ is a random number following the Bernoulli distribution with equal probability as before. Note that, in the proposed solution, the robots do not require any information about the global performance index $J$ because $J$ does not appear in (14) nor (15).

The proposed local controller $L_i$ plays a role similar to that of the chemotaxis controller $K$. Because $\xi_i(t) = J_i([\boldsymbol{x}_j(t-1)]_{j\in\mathbb{N}_i(t-1)})$ from (2) and (14), the state $\xi_i(t)$ stores the value of the local performance index at the previous time step. Thus, $\xi_i(t) \le J_i([\boldsymbol{x}_j(t)]_{j\in\mathbb{N}_i(t)})$ indicates that the current local performance is higher than or equal to the previous one. In this case, $L_i$ moves robot $i$ in the current direction. In contrast, $\xi_i(t) > J_i([\boldsymbol{x}_j(t)]_{j\in\mathbb{N}_i(t)})$ indicates that the current local performance is lower than the previous one. In this case, $L_i$ rotates robot $i$ $(2/3)\pi$ radians and moves it forward. The rotation direction is randomly chosen by $w_i(t)$. In this manner, $L_i$ moves robot $i$ so as to increase $J_i$. As a result, $J$ increases according to condition (C2), and coverage will be achieved.

*Remark 2:* We assume that each robot has information about the target coverage space $\mathbb{Q}$, but it is possible to use the proposed controllers even in cases where this information is not given. In fact, if each robot $i$ can detect the boundary of $\mathbb{Q}$ within radius $r/2$, it can calculate the value of the local performance index $J_i$ in (10) because $J_i$ expresses the area of the region that is only covered by robot $i$, as mentioned in the proof of Theorem 1.

*Remark 3:* The proposed controllers can be extended to cases wherein the desired configuration of the robots is non-uniform. This can be performed by introducing a weighting function corresponding to the desired distribution to the target coverage space $\mathbb{Q}$ and by replacing "1" in the integrals in (4) and (10) with the weighting function. That is, let

$$J(\boldsymbol{x}) := \int_{\mathbb{Q}\cap(\cup_{i=1}^n \mathbb{B}(\boldsymbol{x}_i, r/2))} \phi(\boldsymbol{q})\, d\boldsymbol{q}, \tag{16}$$

$$J_i([\boldsymbol{x}_j]_{j\in\mathbb{N}_i}) := \int_{\mathbb{Q}\cap(\cup_{j\in\mathbb{N}_i}\mathbb{B}(\boldsymbol{x}_j, r/2))} \phi(\boldsymbol{q})\, d\boldsymbol{q} - \int_{\mathbb{Q}\cap(\cup_{j\in\mathbb{N}_i\setminus\{i\}}\mathbb{B}(\boldsymbol{x}_j, r/2))} \phi(\boldsymbol{q})\, d\boldsymbol{q} \quad (i = 1, 2, \ldots, n), \tag{17}$$

where $\phi : \mathbb{Q} \to \mathbb{R}_{0+}$ is the weighting function.

### C. NUMERICAL AND EXPERIMENTAL EVALUATIONS

#### 1) NUMERICAL SIMULATION

Consider the multi-robot system shown in Fig. 4 with $n := 6$ and $r := 0.8$. The target coverage space is set as $\mathbb{Q} := [0, 2]^2$. We use the local controllers $L_i$ $(i = 1, 2, \ldots, 6)$ given by (2), (10), (14), and (15) with $v := 0.04$. The simulation was performed using MATLAB on a computer with an Intel Core i7-6700 (3.40 GHz) CPU and 32.0 GB of RAM.

Fig. 8 shows the time series of the robot positions, where $x_{i1}$ and $x_{i2}$ are the first and second elements of $x_i$, respectively, and the robots are numbered from one to six. In the figure, the small circles and line segments represent the translational and rotational positions of the robots, respectively, and the large circles represent $\mathbb{B}(\boldsymbol{x}_i, r/2)$ $(i = 1, 2, \ldots, 6)$. The computation time for the entire simulation was approximately 1 sec. In addition, Fig. 9 shows the evolution over time of the performance index $J(\boldsymbol{x}(t))$. These results show that the proposed controllers achieve a good degree of coverage. On the other hand, Fig. 10 shows the evolution over time of the local performance indices $J_i([\boldsymbol{x}_j(t)]_{j\in\mathbb{N}_i(t)})$ $(i = 1, 2, \ldots, 6)$. Each robot moves so as to increase the local performance index for itself.

Next, we compare the proposed controllers with the controllers developed in [33]. Yan *et al.* [33] considered minimizing the cost function

$$H(\boldsymbol{x}) := \sum_{i=1}^{n} \int_{\mathbb{V}_i(\boldsymbol{x})} \|\boldsymbol{q} - \boldsymbol{x}_i\|^2\, d\boldsymbol{q}, \tag{18}$$

where $\mathbb{V}_i(\boldsymbol{x}) \subset \mathbb{Q}$ is the Voronoi cell for robot $i$, defined as

$$\mathbb{V}_i(\boldsymbol{x}) := \{\boldsymbol{q} \in \mathbb{Q} \mid \|\boldsymbol{q} - \boldsymbol{x}_i\| \le \|\boldsymbol{q} - \boldsymbol{x}_j\|\ \forall j \in \{1, 2, \ldots, n\}\} \tag{19}$$

and uniform coverage is assumed. The cost function $H(\boldsymbol{x})$ represents the sum of the integrals of the squared distance between $\boldsymbol{x}_i$ and each point $\boldsymbol{q}$ in $\mathbb{V}_i(\boldsymbol{x})$, and $\mathbb{V}_i(\boldsymbol{x})$ represents the region comprising the points closer to robot $i$ than the others. Therefore, minimizing $H(\boldsymbol{x})$ means coverage in the sense that at least one robot is located near any point in the target coverage space $\mathbb{Q}$. Fig. 11 shows the evolution over

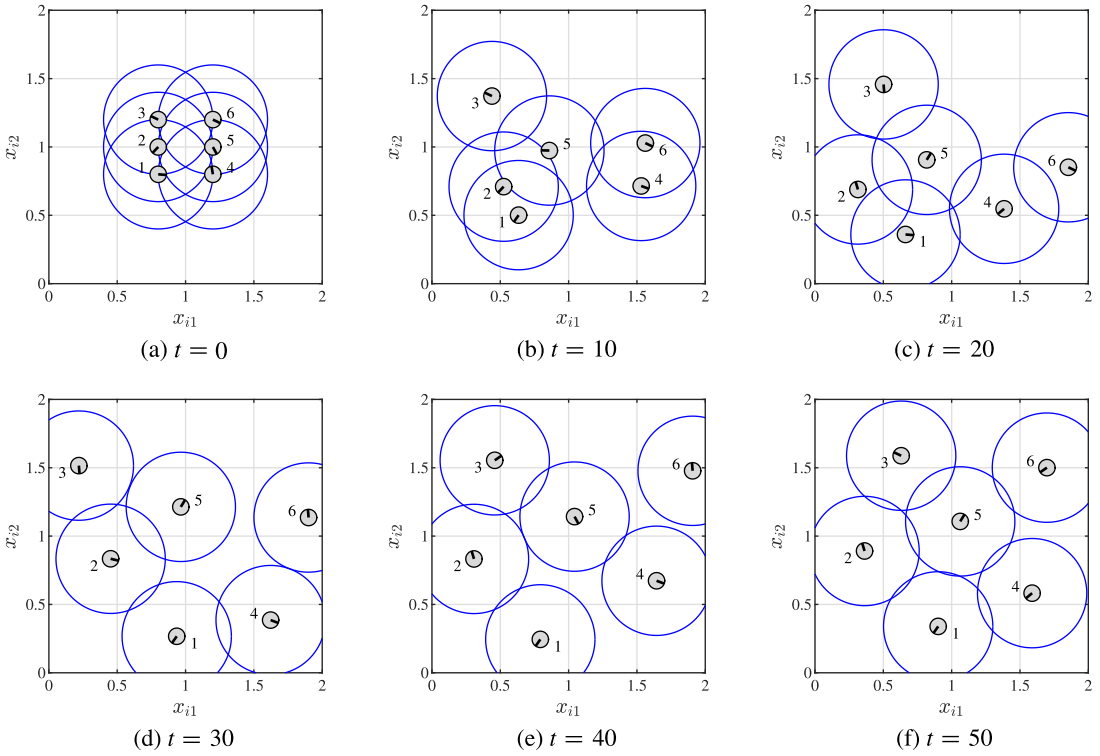


**FIGURE 8.** Simulation result for coverage.

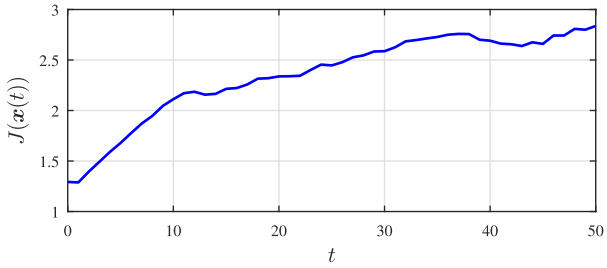


**FIGURE 9.** Time evolution of the performance index $J$.

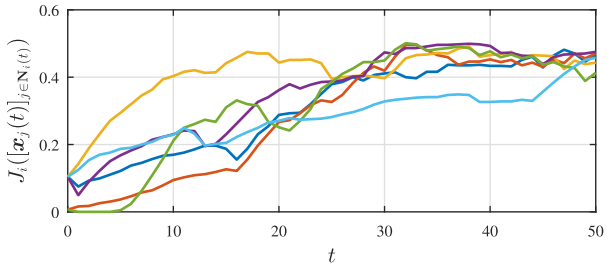


**FIGURE 10.** Time evolution of the local performance indices $J_i$ ($i = 1, 2, \ldots, 6$).

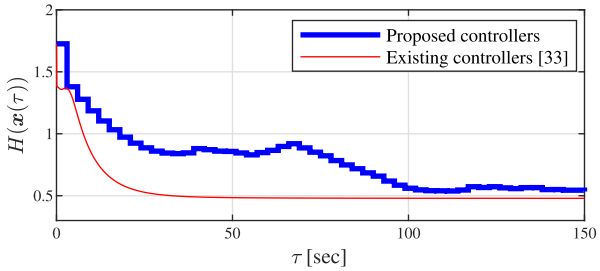


**FIGURE 11.** Time evolution of the cost function $H$.

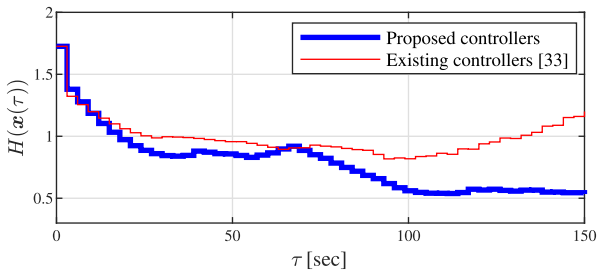


**FIGURE 12.** Time evolution of the cost function $H$ when each control input is quantized.

time of $H(\boldsymbol{x}(\tau))$ for the result in Fig. 8 and that obtained using the controllers given in [33]. Here, considering that a continuous-time system was treated in [33], we introduce the continuous-time variable $\tau \in \mathbb{R}_{0+}$ and count one time step in Fig. 8 as 3 sec based on the experimental results described later. We see from Fig. 11 that compared with the controllers given in [33], the proposed controllers achieve similar performance in terms of the final value of $H(x(\tau))$, but the time needed to complete coverage is long. This is because we use the three types of control inputs only, *i.e.*, $\boldsymbol{u}_i(t) = [v \;\; 0]^\top$, $[v \;\; (2/3)\pi]^\top$, and $[v \;\; -(2/3)\pi]^\top$, from (2) and (15), whereas Yan *et al.* [33] did not. We thus show in Fig. 12 the comparison of the evolution over time of $H(\boldsymbol{x}(\tau))$ when each $\boldsymbol{u}_i(t)$ for the controllers given in [33] is quantized to $[v \;\; 0]^\top$, $[v \;\; (2/3)\pi]^\top$, and $[v \;\; -(2/3)\pi]^\top$ by a rounding procedure. When the control input to each robot is restricted to the three values, the performance of the proposed

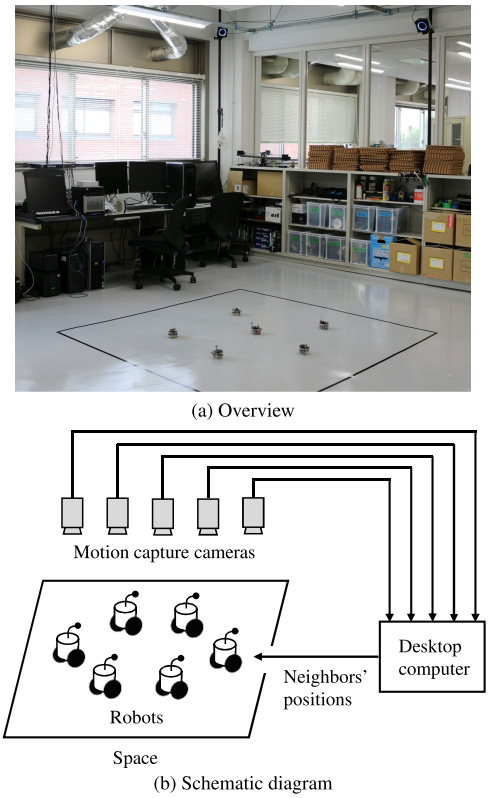


(a) Overview

(b) Schematic diagram

**FIGURE 13.** Experimental setup.

**FIGURE 14.** e-puck robot.

controllers is higher than that of the controllers given in [33]. This is an advantage in the applications to low-cost robots and molecular robots described in Section I-A because it is impractical to control them via high-resolution inputs.

#### 2) EXPERIMENT

To verify the effectiveness of the proposed controllers in a real setting, we constructed the experimental system shown in Fig. 13, comprising six robots, five motion capture cameras, and a desktop computer.

The size of the space in which the robots moved was $2 \times 2$ m. As the robots, we used e-puck robots [44], as shown in Fig. 14, whose height and diameter were 60 mm and 75 mm, respectively. Each robot has a microcomputer, on which the local controller $L_i$ was implemented. The cameras used were Prime 17W cameras in the motion capture system OptiTrack [45], having a resolution of $1664 \times 1088$ pixels. The desktop computer processed the camera images and calculated the positions of the robots. Each robot received information on the positions of its neighbors over Bluetooth.

In this experimental system, we addressed coverage. The communication/sensing range $r$, the target coverage space $\mathbb{Q}$, and the local controllers $L_i$ $(i = 1, 2, \ldots, 6)$ were the same as those in the simulation.

Fig. 15 shows snapshots of the robot positions, where the robots are numbered from one to six and one time step corresponds to approximately 3 sec. The proposed controllers achieve a good degree of coverage. Note that different random numbers were used in the simulation and the experiment and thus the trajectories of the robots in the experiment differ from those in the simulation. This result demonstrates that the proposed controllers work well on actual robots with some hardware constraints.

*Remark 4:* An important advantage of the method presented here is that it can handle not only coverage but also other tasks if for each task, an appropriate performance index $J$ and its decomposition $J_i$ $(i = 1, 2, \ldots, n)$ can be found. This point is demonstrated in the next section.

## V. APPLICATION TO RENDEZVOUS

This section presents the application of the proposed method to rendezvous, which is also a fundamental task in multi-robot systems.

### A. RENDEZVOUS PROBLEM

Consider the multi-robot system shown in Fig. 4. The dynamics of robot $i$ is given by (1). The local controller $L_i$ is

$$L_i : \begin{cases} \boldsymbol{\xi}_i(t+1) = \boldsymbol{g}_1(\boldsymbol{\xi}_i(t), [\boldsymbol{x}_j(t) - \boldsymbol{x}_i(t)]_{j\in\mathbb{N}_i(t)}), \\ \boldsymbol{u}_i(t) = \boldsymbol{g}_2(\boldsymbol{\xi}_i(t), [\boldsymbol{x}_j(t) - \boldsymbol{x}_i(t)]_{j\in\mathbb{N}_i(t)}), \end{cases} \tag{20}$$

where $[\boldsymbol{x}_j(t) - \boldsymbol{x}_i(t)]_{j\in\mathbb{N}_i(t)} \in \mathbb{R}^{2|\mathbb{N}_i(t)|}$ is the input. We suppose here that the neighbor set $\mathbb{N}_i(t)$ is the index set of the robots from which robot $i$ can obtain information on *relative* positions. That is, robot $i$ directly obtains information on the difference between $\boldsymbol{x}_j(t)$ and $\boldsymbol{x}_i(t)$. We represent the network structure among the robots via an undirected graph $G = (\mathbb{V}, \mathbb{E})$, where $\mathbb{V} := \{1, 2, \ldots, n\}$ is the vertex set corresponding to the robots and $\mathbb{E} \subset \mathbb{V} \times \mathbb{V}$ is the edge set corresponding to the connections between them. We assume that $G$ is fixed (*i.e.,* time-invariant). Then, the neighbor set is the time-invariant set given by

$$\mathbb{N}_i := \{j \in \{1, 2, \ldots, n\} \mid (i, j) \in \mathbb{E}\}. \tag{21}$$

Rendezvous means that all robots gather at a common point, *i.e.,* $\boldsymbol{x}_1(t) = \boldsymbol{x}_2(t) = \cdots = \boldsymbol{x}_n(t)$ for some $t$. Hence, the problem addressed here is formulated as follows.

*Problem 2:* For the multi-robot system shown in Fig. 4, find local controllers $L_1, L_2, \ldots, L_n$ (*i.e.,* functions $\boldsymbol{g}_1$ and $\boldsymbol{g}_2$) such that

$$\lim_{t\to\infty} (\boldsymbol{x}_i(t) - \boldsymbol{x}_j(t)) = \boldsymbol{0} \quad \forall (i, j) \in \{1, 2, \ldots, n\}^2 \tag{22}$$

for every initial state $(\boldsymbol{x}_i(0), \theta_i(0)) \in \mathbb{R}^2 \times \mathbb{R}$ $(i = 1, 2, \ldots, n)$.

*Remark 5:* We suppose that the robots determine a favorable rendezvous point by negotiating with each other

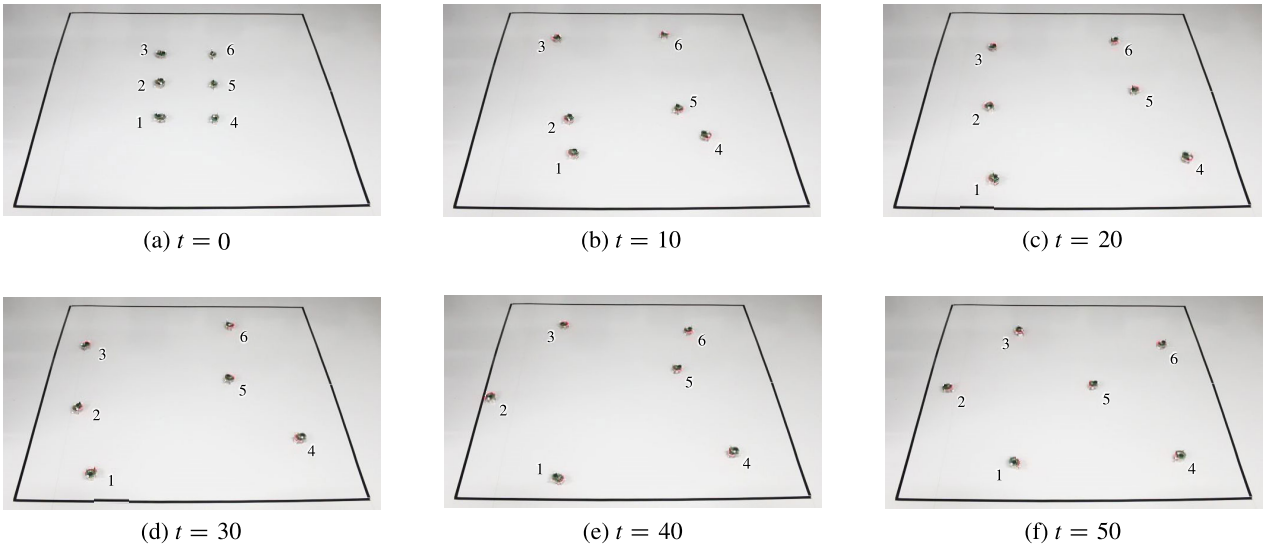

(a) $t = 0$ (b) $t = 10$ (c) $t = 20$

(d) $t = 30$ (e) $t = 40$ (f) $t = 50$

**FIGURE 15.** Experimental result for coverage.

while observing their neighbors, as shown in Fig. 3. Thus, similar to Problem 1, any local controllers whose inputs do not depend on the positions of the neighbors cannot be a solution to Problem 2. Our goal here is to solve the problem by appropriately combining the chemotaxis controller with information on the positions of the neighbors. On the other hand, from the problem setting, one might think that a solution could be obtained via the direct application of the chemotaxis controller for an attractant, but this is not true. In fact, the concentration signal of an attractant is not provided. Moreover, introducing a virtual concentration signal is impossible because each robot $i$ cannot know the relation between its own position and the rendezvous point (corresponding to the location of the attractant) from only $[\boldsymbol{x}_j(t) - \boldsymbol{x}_i(t)]_{j\in\mathbb{N}_i(t)}$; thus, it cannot know the virtual concentration at its current position.

### B. PROPOSED CONTROLLERS

In a manner similar to that described in Section IV, we present a solution to Problem 2. More specifically, we introduce a performance index $J$ for rendezvous and derive its decomposition $J_i$ $(i = 1, 2, \ldots, n)$ by considering the network structure. Subsequently, we combine $J_i$ and the chemotaxis controller $K$ in (7).

Based on this idea, we introduce the following performance index:

$$J(\boldsymbol{x}) := -\frac{1}{2}\sum_{i=1}^{n}\sum_{j\in\mathbb{N}_i}\|\boldsymbol{x}_i - \boldsymbol{x}_j\|, \tag{23}$$

and also consider the following local indices:

$$J_i([\boldsymbol{x}_j - \boldsymbol{x}_i]_{j\in\mathbb{N}_i}) := -\sum_{j\in\mathbb{N}_i}\|\boldsymbol{x}_j - \boldsymbol{x}_i\| \quad (i = 1, 2, \ldots, n). \tag{24}$$

Then, the following result is obtained.

*Theorem 2:* Consider the performance index $J$ in (23) and the local performance index $J_i$ in (24). Then, the following statements hold.

(i) Assume that the graph $G$ is connected. If $J(\boldsymbol{x}) = 0$, then $\boldsymbol{x}_i - \boldsymbol{x}_j = \boldsymbol{0}$ for every $(i, j) \in \{1, 2, \ldots, n\}^2$.
(ii) Condition (C1) holds (with respect to the relative positions, *i.e.*, $[\boldsymbol{x}_j - \boldsymbol{x}_i]_{j\in\mathbb{N}_i}$) for every $i \in \{1, 2, \ldots, n\}$.
(iii) (11) holds for every $i \in \{1, 2, \ldots, n\}$.

*Proof:* Statement (i) follows from (23) and the assumption that $G$ is connected. Statement (ii) is trivial from the definition of $J_i$. Finally, (iii) can be proven as follows. From (24), the relation

$$J_i([\boldsymbol{x}_j - \boldsymbol{x}_i]_{j\in\mathbb{N}_i}) + \sum_{j\neq i} J_j([\boldsymbol{x}_k - \boldsymbol{x}_j]_{k\in\mathbb{N}_j}) = -\sum_{i=1}^{n}\sum_{j\in\mathbb{N}_i}\|\boldsymbol{x}_j - \boldsymbol{x}_i\| \tag{25}$$

holds. This and (24) provide

$$\begin{aligned} &J_i([\boldsymbol{x}_j - \boldsymbol{x}_i]_{j\in\mathbb{N}_i}) \\ &= -\sum_{i=1}^{n}\sum_{j\in\mathbb{N}_i}\|\boldsymbol{x}_j - \boldsymbol{x}_i\| - \sum_{j\neq i} J_j([\boldsymbol{x}_k - \boldsymbol{x}_j]_{k\in\mathbb{N}_j}) \\ &= -\sum_{i=1}^{n}\sum_{j\in\mathbb{N}_i}\|\boldsymbol{x}_j - \boldsymbol{x}_i\| + \sum_{j\neq i}\sum_{k\in\mathbb{N}_j}\|\boldsymbol{x}_k - \boldsymbol{x}_j\| \\ &= -\sum_{i=1}^{n}\sum_{j\in\mathbb{N}_i}\|\boldsymbol{x}_j - \boldsymbol{x}_i\| + \sum_{j\neq i}\sum_{k\in\mathbb{N}_j\setminus\{i\}}\|\boldsymbol{x}_k - \boldsymbol{x}_j\| \\ &\quad + \sum_{k\in\mathbb{N}_i}\|\boldsymbol{x}_k - \boldsymbol{x}_i\|, \end{aligned} \tag{26}$$

where we exploit the fact that $G$ is undirected, in order to derive the last equality. By applying (24) to (26), we obtain

$$\begin{aligned} &J_i([\boldsymbol{x}_j - \boldsymbol{x}_i]_{j\in\mathbb{N}_i}) \\ &= -\frac{1}{2}\sum_{j=1}^{n}\sum_{k\in\mathbb{N}_j}\|\boldsymbol{x}_k - \boldsymbol{x}_j\| + \frac{1}{2}\sum_{j\neq i}\sum_{k\in\mathbb{N}_j\setminus\{i\}}\|\boldsymbol{x}_k - \boldsymbol{x}_j\|, \end{aligned} \tag{27}$$

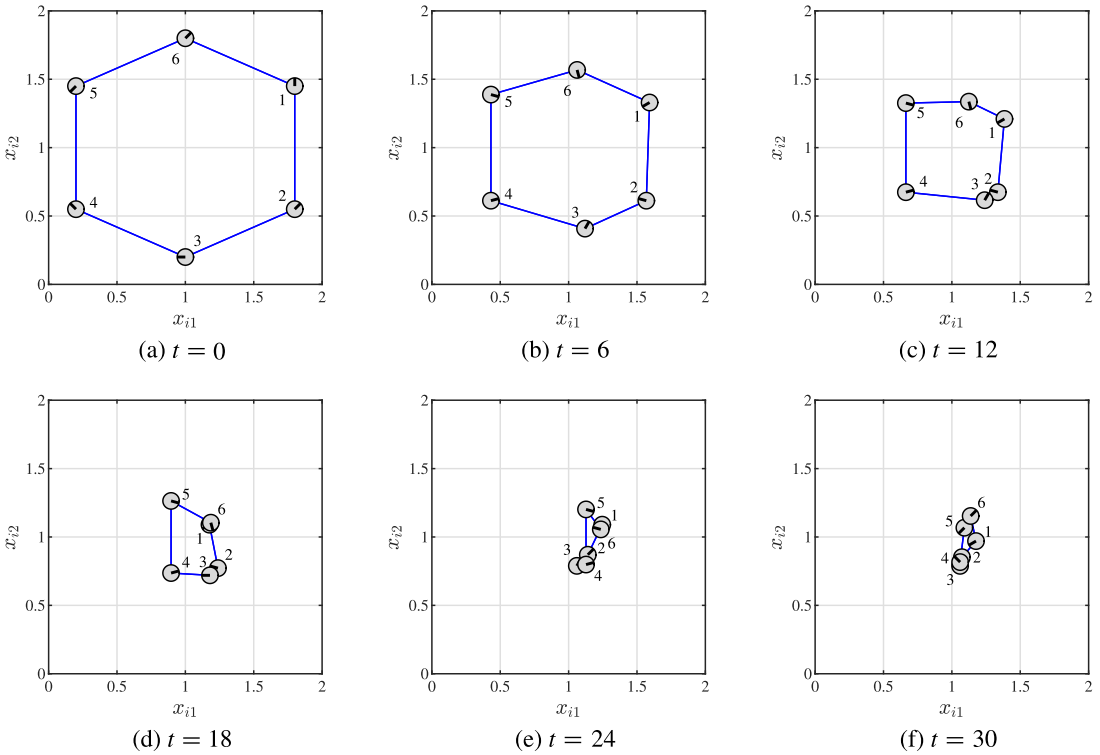


**FIGURE 16.** Simulation result for rendezvous.

where some indices are modified. Therefore, it follows from a property of norm and (23) that

$$J(\boldsymbol{x}) = J_i([\boldsymbol{x}_j - \boldsymbol{x}_i]_{j\in\mathbb{N}_i}) - \frac{1}{2}\sum_{j\neq i}\sum_{k\in\mathbb{N}_j\setminus\{i\}} \|\boldsymbol{x}_k - \boldsymbol{x}_j\|. \qquad (28)$$

By noting that $G$ is fixed, we can show that the second term of the right-hand side of (28) is independent of $\boldsymbol{x}_i$. This and (28) prove (iii). ■

Theorem 2 indicates that $J$ in (23) and $J_i$ in (24) are appropriate for rendezvous. In fact, (i) guarantees that rendezvous is achieved by maximizing $J$ if the graph $G$ is connected. Moreover, (ii) and (iii) imply that $J_i$ ($i = 1, 2, \ldots, n$) are a decomposition of $J$.

From these results, we propose (14), (15), and (24) as a solution to Problem 2. Similar to the case of coverage, each resulting local controller $L_i$ moves robot $i$ so as to increase $J_i$. As a result, $J$ increases according to condition (C2), and rendezvous will be achieved if the graph $G$ is connected.

### C. NUMERICAL AND EXPERIMENTAL EVALUATIONS

Consider the multi-robot system shown in Fig. 4 with $n := 6$. The graph $G$ is given so that it is fixed and connected, as explained later. We employ the local controllers $L_i$ ($i = 1, 2, \ldots, 6$) given by (14), (15), (20), and (24) with $v := 0.04$. The simulation environment was the same as that used for coverage.

Fig. 16 shows the time series of the robot positions in the same manner as in Fig. 8, where the lines between the robots show the edges of the graph $G$. The computation time was approximately 1 sec. We see from Fig. 16 that rendezvous is achieved using the proposed controllers.

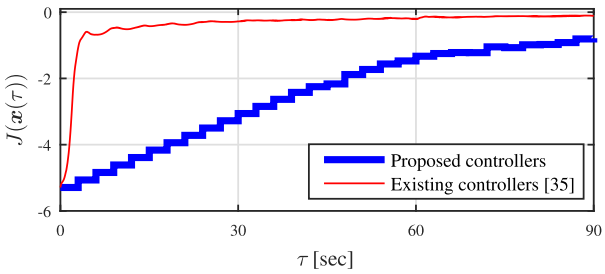


**FIGURE 17.** Time evolution of the performance index $J$ for rendezvous.

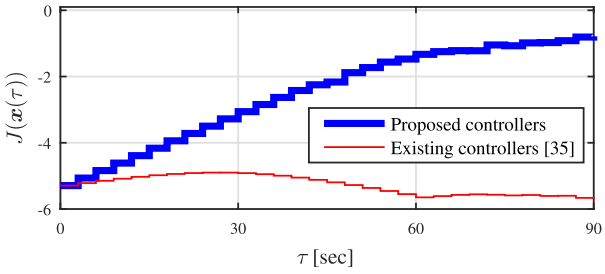


**FIGURE 18.** Time evolution of the performance index $J$ for rendezvous when each control input is quantized.

Next, similar to the case of coverage, we compare the proposed controllers with the controllers developed in [35]. Fig. 17 shows the evolution over time of the performance index $J(\boldsymbol{x}(\tau))$ given by (23) in the same manner as that in Fig. 11. Fig. 18 shows it when each $\boldsymbol{u}_i(t)$ for the controllers given in [35] is quantized to $[v \quad 0]^\top$, $[v \quad (2/3)\pi]^\top$, and $[v \quad -(2/3)\pi]^\top$ by a rounding procedure. These results indicate that unlike the proposed controllers, the controllers given in [35] do not achieve rendezvous when the control input to each robot is restricted to the three values.

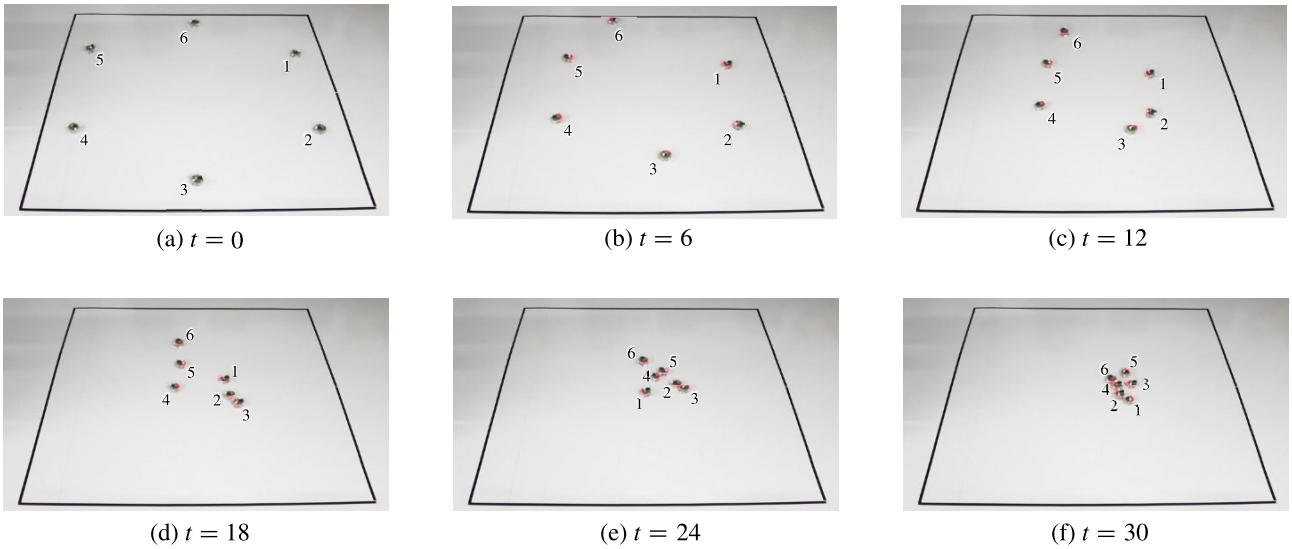

(a) $t = 0$ (b) $t = 6$ (c) $t = 12$

(d) $t = 18$ (e) $t = 24$ (f) $t = 30$

**FIGURE 19.** Experimental result for rendezvous.

**TABLE 3.** Network structures used in our solutions.

| Task | Network structure |
|---|---|
| Coverage | $r$-disk proximity networks |
| Rendezvous | Undirected, fixed, and connected networks |

Moreover, we conducted a validation experiment using the system shown in Fig. 13, where the graph $G$ and the local controllers $L_i$ ($i = 1, 2, \ldots, 6$) were the same as those used in the simulation. Fig. 19 shows the snapshots of the robot positions in the same manner as in Fig. 15, where one time step corresponds to approximately 3 sec. It is apparent that rendezvous is achieved in the experiment using the proposed controllers.

*Remark 6:* Table 3 summarizes the network structures used in our solutions, which are important aspects of this study. In fact, it is necessary to employ the properties of these network structures to prove Theorems 1 and 2. In addition, from the fact that similar network structures can be found in, *e.g.,* [42], even when using a chemotaxis controller, networks similar to those for conventional artificial controllers should be constructed.

## VI. CONCLUSION

In this study, we considered multi-robot coordination via the networking of the chemotaxis controllers of *E. coli*. By regarding the performance index quantifying the achieved degree of the task as the concentration of a chemical for chemotaxis, we obtained networked controllers for coverage and rendezvous using the chemotaxis controllers. The performance of the proposed controllers was demonstrated via experiments using mobile robots as well as simulations. These results can possibly lead to new applications of chemotaxis controllers.

In a future study, we plan to obtain theoretical results for the proposed controllers. In particular, we will theoretically analyze their convergence and performance in some stochastic sense.

## REFERENCES


[1] M. Senanayake, I. Senthooran, J. C. Barca, H. Chung, J. Kamruzzaman, and M. Murshed, "Search and tracking algorithms for swarms of robots: A survey," *Robot. Auto. Syst.*, vol. 75, pp. 422–434, Jan. 2016.

[2] H. Oh, A. Ramezan Shirazi, C. Sun, and Y. Jin, "Bio-inspired self-organising multi-robot pattern formation: A review," *Robot. Auto. Syst.*, vol. 91, pp. 83–100, May 2017.

[3] N. R. Hoff, A. Sagoff, R. J. Wood, and R. Nagpal, "Two foraging algorithms for robot swarms using only local communication," in *Proc. IEEE Int. Conf. Robot. Biomimetics*, Dec. 2010, pp. 123–130.

[4] A. Jevtic, Á. Gutierrez, D. Andina, and M. Jamshidi, "Distributed bees algorithm for task allocation in swarm of robots," *IEEE Syst. J.*, vol. 6, no. 2, pp. 296–304, Jun. 2012.

[5] J. Pugh and A. Martinoli, "Inspiring and modeling multi-robot search with particle swarm optimization," in *Proc. IEEE Swarm Intell. Symp.*, Apr. 2007, pp. 332–339.

[6] J. Yang, X. Wang, and P. Bauer, "V-shaped formation control for robotic swarms constrained by field of view," *Appl. Sci.*, vol. 8, no. 11, p. 2120, Nov. 2018.

[7] J. Adler, "Chemotaxis in bacteria," *Science*, vol. 153, no. 3737, pp. 708–716, Aug. 1966.

[8] H. C. Berg and D. A. Brown, "Chemotaxis in Escherichia coli analysed by three-dimensional tracking," *Nature*, vol. 239, no. 5374, pp. 500–504, Oct. 1972.

[9] W.-W. Tso and J. Adler, "Negative chemotaxis in Escherichia coli," *J. Bacteriology*, vol. 118, no. 2, pp. 560–576, 1974.

[10] S. Murata, A. Konagaya, S. Kobayashi, H. Saito, and M. Hagiya, "Molecular robotics: A new paradigm for artifacts," *New Gener. Comput.*, vol. 31, no. 1, pp. 27–45, Jan. 2013.

[11] C. Lytridis, G. S. Virk, Y. Rebour, and E. E. Kadar, "Odor-based navigational strategies for mobile agents," *Adapt. Behav.*, vol. 9, nos. 3–4, pp. 171–187, Sep. 2001.

[12] L. Marques, U. Nunes, and A. T. de Almeida, "Olfaction-based mobile robot navigation," *Thin Solid Films*, vol. 418, no. 1, pp. 51–58, Oct. 2002.

[13] R. A. Russell, A. Bab-Hadiashar, R. L. Shepherd, and G. G. Wallace, "A comparison of reactive robot chemotaxis algorithms," *Robot. Auto. Syst.*, vol. 45, no. 2, pp. 83–97, Nov. 2003.

[14] A. Dhariwal, G. S. Sukhatme, and A. A. G. Requicha, "Bacterium-inspired robots for environmental monitoring," in *Proc. IEEE Int. Conf. Robot. Autom. (ICRA)*, vol. 2, Apr. 2004, pp. 1436–1443.

[15] C. Lytridis, E. E. Kadar, and G. S. Virk, "A systematic approach to the problem of odour source localisation," *Auto. Robots*, vol. 20, no. 3, pp. 261–276, Jun. 2006.

[16] T. Schmickl, H. Hamann, J. Stradner, R. Mayet, and K. Crailsheim, "Complex taxis-behaviour in a novel bio-inspired robot controller," in *Proc. 12th Int. Conf. Simulation Synth. Living Syst.*, Aug. 2010, pp. 648–658.

[17] J. Oyekan and H. Hu, "Bacteria controller implementation on a physical platform for pollution monitoring," in *Proc. IEEE Int. Conf. Robot. Autom.*, May 2010, pp. 3781–3786.

[18] S. G. Nurzaman, Y. Matsumoto, Y. Nakamura, S. Koizumi, and H. Ishiguro, "'Yuragi'-based adaptive mobile robot search with and without gradient sensing: From bacterial chemotaxis to a Levy walk," *Adv. Robot.*, vol. 25, no. 16, pp. 2019–2037, Jan. 2011.
[19] J. Cortes, S. Martinez, T. Karatas, and F. Bullo, "Coverage control for mobile sensing networks," *IEEE Trans. Robot. Autom.*, vol. 20, no. 2, pp. 243–255, Apr. 2004.
[20] R. Olfati-Saber, J. A. Fax, and R. M. Murray, "Consensus and cooperation in networked multi-agent systems," *Proc. IEEE*, vol. 95, no. 1, pp. 215–233, Jan. 2007.
[21] N. Samways, Y. Jin, X. Yao, and B. Sendhoff, "Toward a gene regulatory network model for evolving chemotaxis behavior," in *Proc. IEEE Congr. Evol. Comput. (IEEE World Congr. Comput. Intell.)*, Jun. 2008, pp. 2569–2576.
[22] B. Yang, Y. Ding, Y. Jin, and K. Hao, "Self-organized swarm robot for target search and trapping inspired by bacterial chemotaxis," *Robot. Auto. Syst.*, vol. 72, pp. 83–92, Oct. 2015.
[23] J. Oyekan, H. Hu, and D. Gu, "A novel bio-inspired distributed coverage controller for pollution monitoring," in *Proc. IEEE Int. Conf. Mechatronics Autom.*, Aug. 2011, pp. 1651–1656.
[24] J. Oyekan, D. Gu, and H. Hu, "Visual imaging of invisible hazardous substances using bacterial inspiration," *IEEE Trans. Syst., Man, Cybern. Syst.*, vol. 43, no. 5, pp. 1105–1115, Sep. 2013.
[25] L. Bai, M. Eyiyurekli, and D. E. Breen, "An emergent system for self-aligning and self-organizing shape primitives," in *Proc. 2nd IEEE Int. Conf. Self-Adapt. Self-Organizing Syst.*, Oct. 2008, pp. 445–454.
[26] S. Grimes, L. Bai, A. W. E. McDonald, and D. E. Breen, "Directing chemotaxis-based spatial self-organisation via biased, random initial conditions," *Int. J. Parallel, Emergent Distrib. Syst.*, vol. 34, no. 4, pp. 380–399, Jul. 2019.
[27] N. Fatès and N. Vlassopoulos, "A robust aggregation method for quasi-blind robots in an active environment," in *Proc. Int. Conf. Swarm Intell.*, Jun. 2011, pp. 1–10.
[28] M. Eyiyurekli, L. Bai, P. I. Lelkes, and D. E. Breen, "Chemotaxis-based sorting of self-organizing heterotypic agents," in *Proc. ACM Symp. Appl. Comput. (SAC)*, 2010, pp. 1315–1322.
[29] L. Bai, M. Eyiyurekli, P. I. Lelkes, and D. E. Breen, "Self-organized sorting of heterotypic agents via a chemotaxis paradigm," *Sci. Comput. Program.*, vol. 78, no. 5, pp. 594–611, May 2013.
[30] A. Kwok and S. Martinez, "Unicycle coverage control via hybrid modeling," *IEEE Trans. Autom. Control*, vol. 55, no. 2, pp. 528–532, Feb. 2010.
[31] J.-M. Luna, R. Fierro, C. Abdallah, and J. Wood, "An adaptive coverage control algorithm for deployment of nonholonomic mobile sensors," in *Proc. 49th IEEE Conf. Decis. Control (CDC)*, Dec. 2010, pp. 1250–1256.
[32] Q. Liu, M. Ye, Z. Sun, J. Qin, and C. Yu, "Coverage control of unicycle agents under constant speed constraints," *IFAC-PapersOnLine*, vol. 50, no. 1, pp. 2471–2476, Jul. 2017.
[33] M. Yan, Y. Guo, L. Zuo, and P. Yang, "Information-based optimal deployment for a group of dynamic unicycles," *Int. J. Control, Autom. Syst.*, vol. 16, no. 4, pp. 1824–1832, Jul. 2018.
[34] D. V. Dimarogonas and K. J. Kyriakopoulos, "On the rendezvous problem for multiple nonholonomic agents," *IEEE Trans. Autom. Control*, vol. 52, no. 5, pp. 916–922, May 2007.
[35] N. Zoghlami, R. Mlayeh, L. Beji, and A. Abichou, "Finite-time consensus for controlled dynamical systems in network," *Int. J. Control*, vol. 91, no. 4, pp. 813–826, Apr. 2018.
[36] K.-C. Cao, B. Jiang, and D. Yue, "Rendezvous of multiple nonholonomic unicycles-based on backstepping," *Int. J. Control*, vol. 91, no. 6, pp. 1271–1283, Jun. 2018.
[37] S. Zhao, D. V. Dimarogonas, Z. Sun, and D. Bauso, "A general approach to coordination control of mobile agents with motion constraints," *IEEE Trans. Autom. Control*, vol. 63, no. 5, pp. 1509–1516, May 2018.
[38] A. Ozdemir, M. Gauci, A. Kolling, M. D. Hall, and R. Gros, "Spatial coverage without computation," in *Proc. Int. Conf. Robot. Autom. (ICRA)*, May 2019, pp. 9674–9680.
[39] J. R. Marden, G. Arslan, and J. S. Shamma, "Cooperative control and potential games," *IEEE Trans. Syst., Man, Cybern., B, Cybern.*, vol. 39, no. 6, pp. 1393–1407, Dec. 2009.
[40] S. Izumi, S.-I. Azuma, and T. Sugie, "Coverage control inspired by bacterial chemotaxis," in *Proc. IEEE 33rd Int. Symp. Reliable Distrib. Syst. Workshops*, Oct. 2014, pp. 34–39.
[41] S. Izumi and S.-I. Azuma, "Chemotaxis-inspired control for multi-agent coordination: Formation control by two types of chemotaxis controllers," *New Gener. Comput.*, vol. 38, pp. 303–324, May 2020.
[42] S. Martinez, J. Cortes, and F. Bullo, "Motion coordination with distributed information," *IEEE Control Syst. Mag.*, vol. 27, no. 4, pp. 75–88, Aug. 2007.
[43] S.-I. Azuma, K. Owaki, N. Shinohara, and T. Sugie, "Performance analysis of chemotaxis controllers: Which has better chemotaxis controller, Escherichia coli or Paramecium caudatum?" *IEEE/ACM Trans. Comput. Biol. Bioinf.*, vol. 13, no. 4, pp. 730–741, Jul. 2016.
[44] F. Mondada, M. Bonani, X. Raemy, J. Pugh, C. Cianci, A. Klaptocz, S. Magnenat, J.-C. Zufferey, D. Floreano, and A. Martinoli, "The e-puck, a robot designed for education in engineering," in *Proc. 9th Conf. Auton. Robot Syst. Compet.*, May 2009, vol. 1, no. 1, pp. 59–65.
[45] NaturalPoint, Corvallis, OR, USA. *OptiTrack*. Accessed: May 29, 2020. [Online]. Available: http://www.optitrack.com/

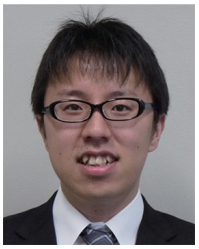

**SHINSAKU IZUMI** (Member, IEEE) received the M.S. and Ph.D. degrees in informatics from Kyoto University, Japan, in 2012 and 2015, respectively. He is currently an Assistant Professor with the Faculty of Computer Science and Systems Engineering, Okayama Prefectural University, Japan. His research interests include networked control systems and multi-agent systems.

**SHUN-ICHI AZUMA** (Senior Member, IEEE) was born in Tokyo, Japan, in 1976. He received the B.Eng. degree in electrical engineering from Hiroshima University, Higashihiroshima, Japan, in 1999, and the M.Eng. and Ph.D. degrees in control engineering from the Tokyo Institute of Technology, Tokyo, in 2001 and 2004, respectively. Prior to joining Nagoya University, he was an Assistant Professor and an Associate Professor with the Department of Systems Science, Graduate School of Informatics, Kyoto University at Uji Campus, Kyoto, Japan, from 2005 to 2011 and from 2011 to 2017, respectively. He is currently a Professor with the Department of Mechanical Systems Engineering, Graduate School of Engineering, Nagoya University, Nagoya, Japan. His research interests include hybrid systems and networked systems. He has been serving as an Associate Editor for the IEEE TRANSACTIONS ON CONTROL OF NETWORK SYSTEMS, since 2013, *Automatica* (IFAC), since 2014, the IEEE CONTROL SYSTEMS LETTERS, since 2016, and *Nonlinear Analysis: Hybrid Systems*, since 2017.

**TOSHIHARU SUGIE** (Fellow, IEEE) received the B.E., M.E., and Ph.D. degrees in engineering from Kyoto University, Japan, in 1976, 1978, and 1985, respectively. From 1978 to 1980, he was a Research Member of the Musashino Electric Communication Laboratory, NTT Musashino, Japan. From 1984 to 1988, he was a Research Associate with the Department of Mechanical Engineering, Osaka Prefecture University, Osaka. From 1988 to 2019, he worked at Kyoto University, where he has been a Professor with the Department of Systems Science, since 1997. In 2019, he joined the Komatsu MIRAI Construction Equipment Cooperative Research Center, Graduate School of Engineering, Osaka University, as a Research Member. His research interests are in robust control, identification for control, and control applications to mechanical systems. He served as an Editor for *Automatica* and was also an Associate Editor for the *Asian Journal of Control* and the *International Journal of Systems Science*.